Application of simultaneous inversion of velocity and angle-dependent reflectivity in frontier exploration

Nizar Chemingui[1]*, Sriram Arasanipalai[1], Cyrille Reiser[1], Sean Crawley[1], Mariana Gherasim[1], Jaime Ramos-Martinez[1] and Guanghui Huang[1] describe how a simultaneous velocity and angle-dependent reflectivity inversion workflow can provide accurate and high-resolution attributes that could help derisk frontier exploration.

Introduction

Seismic attributes can play a crucial role in hydrocarbon exploration by identifying potential prospects. Therefore, seismic inversion has proven to be an effective approach for generating earth models, which are then used for attribute calculations to aid interpretation. We previously introduced a novel seismic inversion technique for the joint estimation of velocity and reflectivity (Yang et al., 2022). This solution employs a vector reflectivity parameterisation of the wave equation (Whitmore et al., 2021) and uses efficient scale separation as the basis for the simultaneous inversion. The scale separation approach, based on inverse scattering theory, has been effectively employed in Reverse Time Migration (RTM) (Whitmore and Crawley, 2012) and Full Waveform Inversion (FWI) (Ramos-Martinez et al., 2016). The new inversion approach enables iterative estimation of both velocity and reflectivity within a single framework, allowing us to derive additional attributes such as relative impedance and density to improve prospectivity assessment.

Additionally, seismic amplitude variations with angle can provide valuable insights into fluid content, porosity, and lithology of subsurface formations for a deeper understanding of subsurface geology. However, conventional solutions for FWI do not straightforwardly compute pre-stack reflectivity, which is crucial for Amplitude Versus Angle (AVA) analysis.

In this work, we expand on our simultaneous inversion workflow which updates velocity and stacked 3D reflectivity, by incorporating angle and azimuth-dependent pre-stack reflectivity (Chemingui et. al, 2023). Our method extracts geometric information from the vector reflectivity and the pressure wavefield as it propagates in the earth's subsurface. This enables us to compute the angle between the incident wavefield and the vector reflectivity, thereby facilitating the construction of angle gathers. During the simultaneous inversion process, the velocity model and angle gathers are continuously updated, leading to improved model resolution and compensating for incomplete acquisition and variations in illumination.

We demonstrate the application of our simultaneous inversion workflow using 3D seismic data from the frontier Salar and Orphan Basins, offshore Newfoundland and Labrador, Canada. This approach yields more reliable attributes and better insight into prospectivity, which can help derisk exploration efforts in these frontier areas.

Methodology – Simultaneous inversion of velocity and angle-dependent reflectivity

In general, seismic inversion relies on a modelling relation defined by the wave equation, which connects the recorded seismic data to subsurface models. The process involves iteratively adjusting model parameters to minimise discrepancies between observed and predicted seismic responses. In our formulation, we use the acoustic wave equation, parameterised in terms of velocity and vector reflectivity (Whitmore et al., 2021):

$$\frac{1}{V^2(\boldsymbol{x})}\frac{\partial^2 P(\boldsymbol{x},t)}{\partial t^2}-\nabla^2 P(\boldsymbol{x},t)-\frac{\nabla V(\boldsymbol{x})}{V(\boldsymbol{x})}\cdot\nabla P(\boldsymbol{x},t)+2\boldsymbol{R}(\boldsymbol{x})\cdot\nabla P(\boldsymbol{x},t)=S(\boldsymbol{x},t) \quad (1)$$

In this equation, P represents the pressure wavefield, V denotes the velocity, and R(x) is the vector reflectivity defined as,

$$\boldsymbol{R}(\boldsymbol{x})=\frac{1}{2}\frac{\nabla Z(\boldsymbol{x})}{Z(\boldsymbol{x})} \quad (2)$$

where Z is the acoustic impedance, and the source term is represented by S(x, t).

In the above formulation, velocity and reflectivity are explicitly set as model parameters eliminating the need to construct a density model. The sensitivity kernels for velocity and impedance obtained through inverse scattering theory (Whitmore and Crawley, 2012; Ramos-Martinez et al., 2016), are combined with the special representation of the wave equation, forming the basis for our simultaneous inversion of velocity and reflectivity (Yang et al., 2022).

To construct angle gathers, it is essential to compute the incidence and reflection angles (or reflector dip direction) at each image point. The vector reflectivity wave equation includes a fundamental characteristic that facilitates the calculation of these angles. Specifically, the gradient of the forward propagation

[1] PGS
* Corresponding author, E-mail: nizar.chemingui@pgs.com
DOI: 10.3997/1365-2397.fb2024061

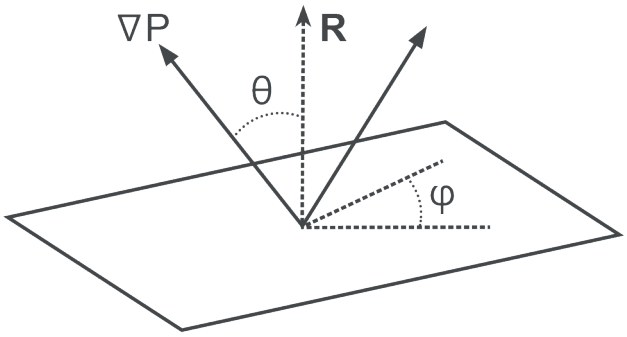

Figure 1 Geometric relation between the vector reflectivity (R), the gradient of the pressure field , and the reflection angle *(θ)* and azimuth *(φ)*.

wavefield provides the incident wavefield's direction, whereas the vector reflectivity contains information about the reflector. Consequently, the reflection angle required for constructing the pre-stack angle gathers can be derived as follows:

$$\theta = \arccos\left(\frac{\boldsymbol{R} \cdot \nabla P}{\|\boldsymbol{R}\| \cdot \|\nabla P\|}\right) \quad (3)$$

Figure 1 illustrates the geometric definition of these elements and their relationship with the reflection angle and its azimuth. The generation of angle gathers follows a process similar to the one used in RTM where angle and azimuth maps are computed for each individual shot and used for the binning of the pre-stack images.

During each iteration, the modelling engine incorporates reflectivity extracted from the current angle gathers, which are continuously updated in subsequent cycles. This process can also produce azimuth gathers by integrating azimuth maps, enabling further characterisation of subsurface structure variations with azimuth.

Application in the Salar Basin – South Bank 3D

The first study area showcasing the benefits of our inversion workflow is in the Salar Basin, located in southeast Newfoundland and Labrador, Canada (Figure 2). The 3D seismic data were acquired in 2020 using multisensor streamer technology. The survey comprised 16 cables with 100 m streamer separation and an 8 km streamer length. Previous analyses of existing seismic data identified several fan systems along the margin, interpreted as Oligocene in age. The main prospectivity is believed to reside in these fans, originating from the shelf and shelf-edge deltas. Within the reservoir interval, Class II AVA anomalies are observed, along with Class IV responses in the deeper section, analogous to a modelled source rock in the region. The average water column depth exceeds 3 km in this area.

In such frontier exploration areas, the lack of well information for calibration of the seismic response puts more demand on optimising the seismic images and their associated attributes in a timely fashion to identify and derisk prospects as efficiently as possible. Therefore, the primary goal of this study was to develop a detailed, high-resolution velocity model to better define the target fan system. The aim was to refine the velocity over the lead and provide reliable pre-stack angle-dependent reflectivity for enhanced interpretative analysis. Successfully achieving these objectives would significantly reduce exploration risks in this basin.

The simultaneous inversion workflow started with a smoothed tomographic velocity model and minimally processed field (shot-ordered) data. A maximum frequency of 40 Hz was selected to delineate the stacked sands in the reservoir interval. Figure 3 shows examples of the starting and inverted models, demonstrating significantly improved resolution of the velocity field resulting from the simultaneous inversion. In addition to the inverted velocity, angle-dependent reflectivity volumes were simultaneously produced. A comparison with similar volumes from a conventional Kirchhoff migration reveals consistent amplitude behaviour and an improved signal-to-noise ratio in the inverted angle gathers (see Figure 4).

The availability of prestack reflectivity volumes from simultaneous inversion enabled the estimation of elastic properties such as relative acoustic impedance and relative Vp/Vs. The relative attributes calculated from the simultaneous inversion are similar and exhibit improved resolution over the main leads in the Tertiary section compared to the attributes from the Kirchhoff migration (Figure 5). The similarity in the computed attributes is reassuring as Kirchhoff migration has long been accepted as an AVA-friendly migration solution.

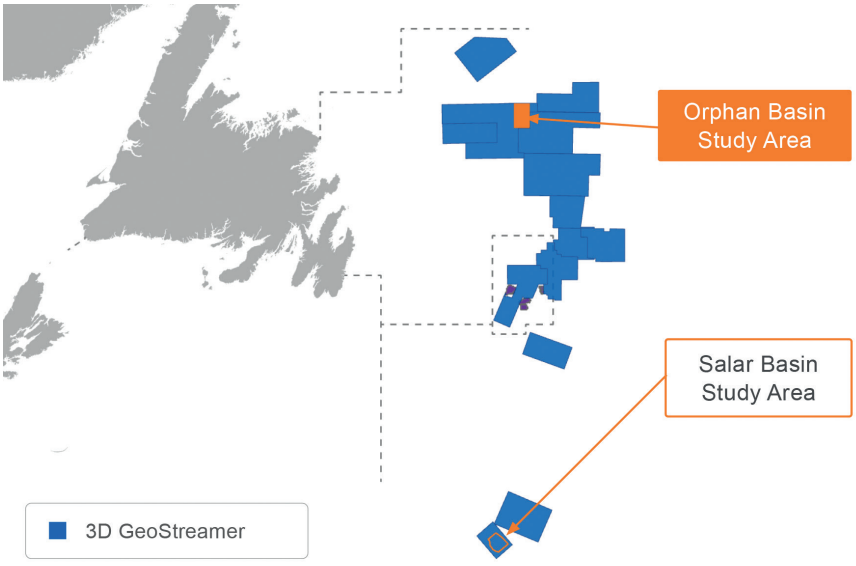

Figure 2 Map showing the study areas in the Salar and Orphan basins, offshore Newfoundland and Labrador.

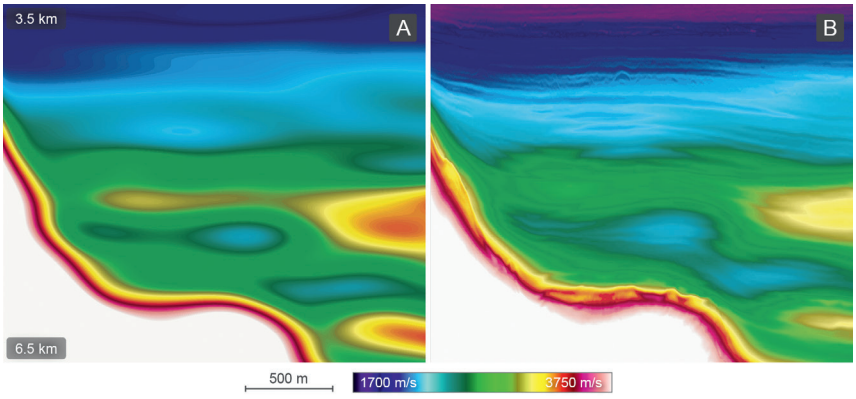

Figure 3 Salar Basin: Example of starting (A) and 40 Hz inverted (B) velocity models. The resolution of the velocity field has significantly improved after the simultaneous inversion, clearly defining the details along the stacked sands.

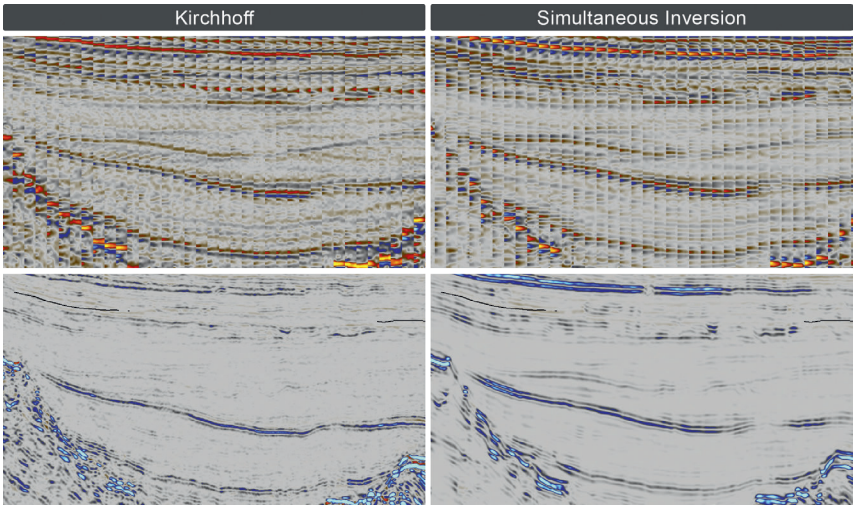

Figure 4 Salar Basin: Comparison of angle gathers from Kirchhoff migration and simultaneous inversion (top row) and the product stack (multiplication of the estimated Shuey 2 term intercept and gradient) (bottom row). Note the similarity between the Kirchhoff migration and inversion results, with a clear improvement in the signal-to-noise ratio in the latter.

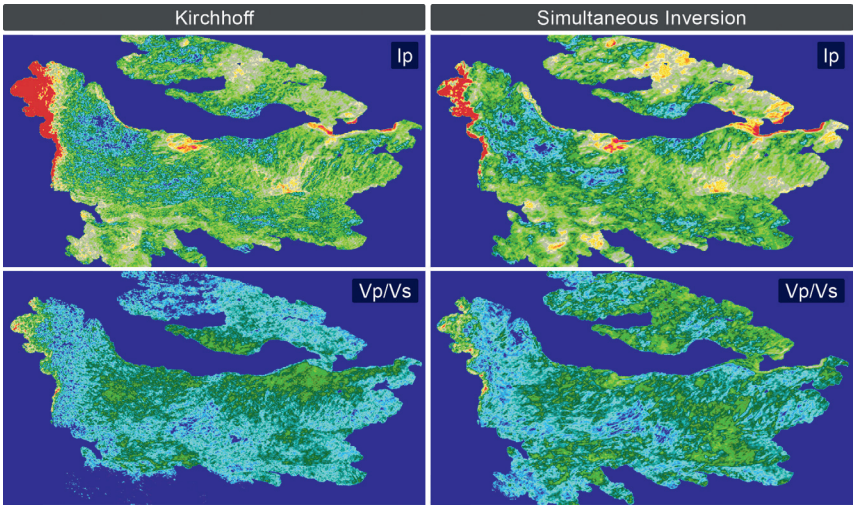

Figure 5 Salar Basin: Example of attribute extraction at the reservoir interval, showing relative acoustic impedance (Ip) (top row) and Vp/Vs (bottom row). The elastic attributes from the simultaneous inversion of shot data align with the results from the conventional Kirchhoff imaging workflow. However, direct inversion from data to seismic attributes significantly reduces the cycle time for building ground models.

Application in the Orphan Basin – Cape Anguille 3D survey

The second study area demonstrating the advantages of our simultaneous inversion is in the Orphan Basin, a highly prospective and underexplored area offshore Newfoundland and Labrador, Canada. Previous exploration endeavours in this basin focused on structural highs in the Cretaceous and Jurassic intervals with limited success. However, the availability of modern, high-quality, 3D regional seismic data has significantly enhanced our understanding of this frontier basin (McCallum et al., 2017). Exploration targets now encompass Late Jurassic and Early Cretaceous reservoirs potentially sourced by Late Jurassic marine shales. Notably, Class II AVA anomalies are observed in the reservoir interval.

The contributing Cape Anguille 3D survey for this study was acquired in 2021 using multisensor streamer technology. This narrow azimuth data was acquired using 16 cables, 100 m streamer separation and 8-km streamer length with water depths around 2 km over the area of interest. The objective of this study was to improve the structural image of the Cretaceous and Jurassic sections at approximate depths of 5-7 km, while appropriately resolving the velocities of the stacked sands in

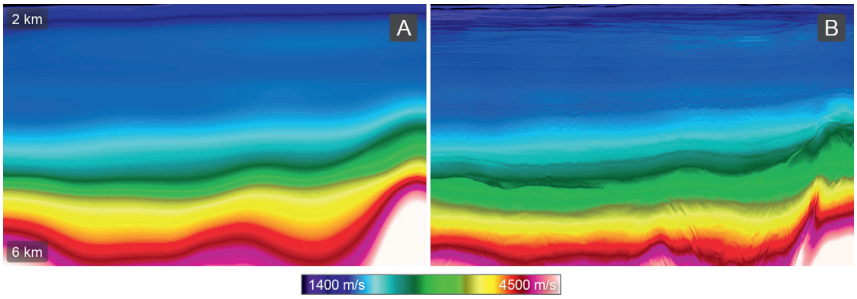

Figure 6 Orphan Basin: Comparison of starting (A) and inverted (B) velocity models. The inverted velocity model shows significant detail over the stacked sands in the reservoir interval (4 km-5 km in depth).

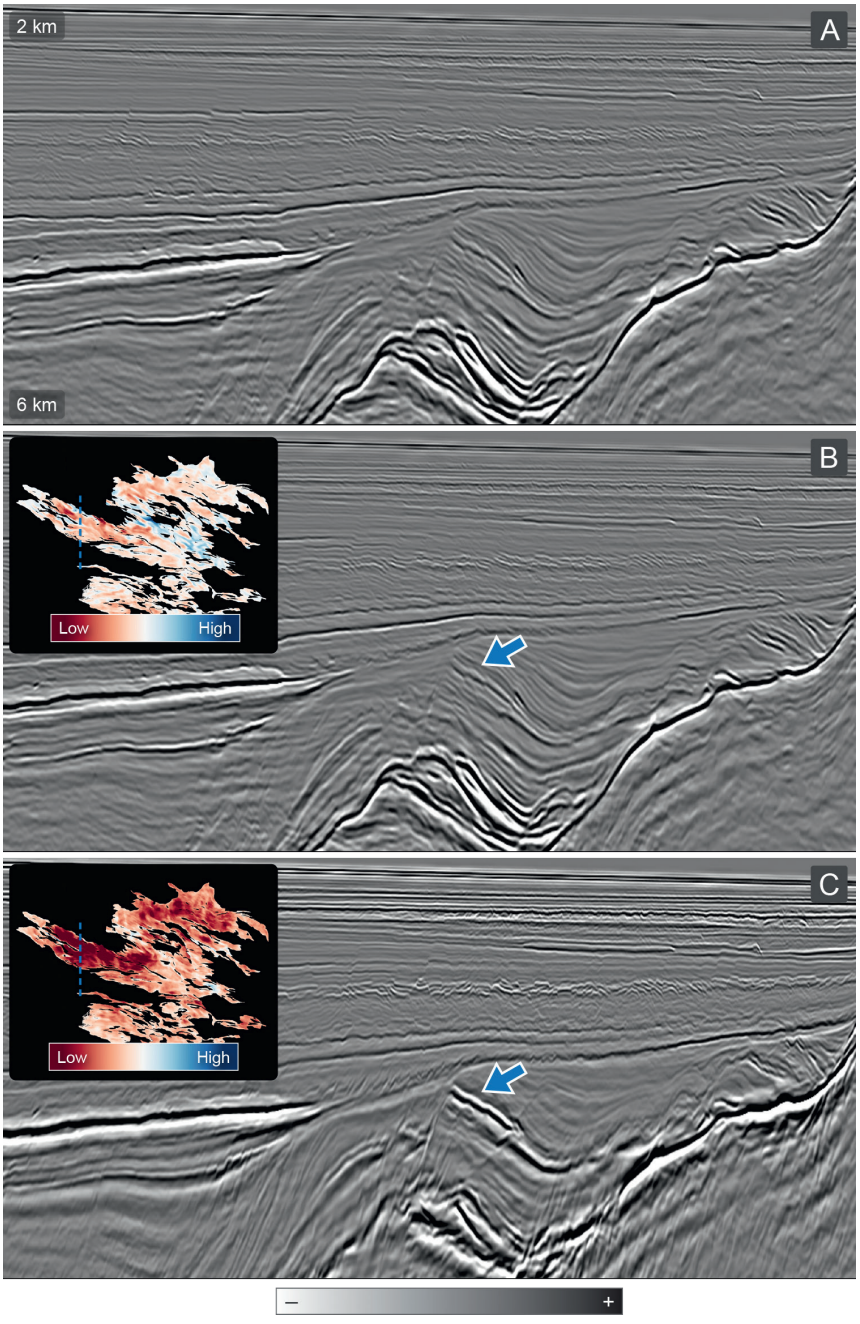

Figure 7 Orphan Basin: A) Full-Stack Reflectivity. B) Near-Angle Stack Reflectivity. C) Far-Angle Stack Reflectivity. The insets in B and C show the amplitudes along a horizon following the top of the lead (blue arrow), highlighting the Class II AVA behaviour.

the Cretaceous basin. One of the challenges identified in the conventional imaging workflow was that remnant multiples compromised the estimation of reliable velocities in the reservoir interval, negatively affecting the structural image. Therefore, a simultaneous inversion workflow was selected to better manage the multiple energy in the recorded data, leading to a more accurate understanding of the potential petroleum system in this basin.

A 40 Hz simultaneous inversion was performed over the study area, outputting inverted velocity and angle-dependent reflectivity volumes, similar to the approach used in the Salar basin described

above. The initial lower-frequency inversions utilised raw hydrophone data, and the starting velocity model was a smoothed tomographic model. The vector reflectivity parameterisation of the wave equation in the simultaneous inversion workflow enables reliable modelling of both primaries and multiples, aiding in the estimation of accurate background velocities in areas affected by multiple energy contamination. Essentially, using data closer to what was acquired in the field helped to build a reliable background velocity model. This approach significantly impacts project turnaround times and exploration decisions. Figure 6 presents a comparison between the 40 Hz inverted velocity model and the starting model. The simultaneous inversion workflow yielded a high-resolution velocity model, revealing intricate details and delineating various sections within the reservoir interval.

The full-stack reflectivity volume output from the simultaneous inversion reveals a detailed section with a robust structural image below the unconformity in the reservoir section at around 5 km depth (Figure 7a). This full reflectivity stack represents the sum of all angles at each image point. The image quality can be further enhanced by excluding non-specular angles, especially in the deeper sections. A comparison of amplitudes over a horizon in the target interval from near and far angle reflectivity volumes illustrates the expected Class II AVA behaviour (Figures 7B and 7C).

Discussion

The application of our enhanced simultaneous inversion workflow is demonstrated with field data examples from offshore Newfoundland and Labrador, Canada. These study areas, located in deep-water settings, feature diverse underlying geology and target intervals. Given the acquisition configuration, it is expected that the model updates are primarily driven by reflection energy in the recorded data. Our proposed multi-parameter inversion utilises the full acoustic wavefield through an innovative formulation of the wave equation in terms of velocity and vector reflectivity. This approach allows for the joint updating of velocity and reflectivity while refining the angular information at each image location. The resulting pre-stack reflectivity volumes provide robust structural images with improved focusing and better fault imaging. Additionally, the results demonstrate the expected amplitude fidelity and an improved signal-to-noise ratio compared to conventional Kirchhoff migration.

Our multi-parameter inversion leverages the similarities between Full Waveform Inversion (FWI) and Least-Squares Reverse Time Migration (LS-RTM). By using scale separation based on the inverse scattering imaging condition, velocity and reflectivity are updated with minimal crosstalk between the models, ensuring that reflectivity changes due to density variations are not falsely mapped as velocity updates. With accurately inverted velocity and reflectivity models, we can easily estimate additional properties, such as relative acoustic impedance and relative Vp/Vs, which are crucial for prospectivity analysis and reservoir studies.

Starting with minimally conditioned field data allows for a faster turnaround of reliable products from the inversion. Consequently, the inverted models and derived properties can provide a direct understanding of the petroleum system and facilitate reliable lead identification, ultimately contributing to reducing exploration risk.

Conclusions

We explored the implementation of our simultaneous inversion solution using two field datasets from offshore Newfoundland and Labrador. Our workflow has been enhanced to produce angle gathers at each subsurface image location, defining angle-dependent earth reflectivity. The resulting images exhibit the expected amplitude fidelity and superior signal-to-noise ratio compared to conventional migration-based workflows. Furthermore, the inverted models were utilised to derive additional subsurface attributes such as relative impedance and relative Vp/Vs, thereby enhancing prospectivity analysis.

By employing minimally processed field data and a simple starting velocity model for the inversion, we can expedite the turnaround time from data acquisition to critical exploration drilling decisions. To this point, the technology aids in derisking potential prospects in areas with imaging challenges, yielding notably different yet reliable results compared to conventional processing techniques.

These simultaneous inversion applications were conducted in frontier exploration basins with limited or no well information, constraining calculations to relative attributes from the inverted results. Directly deriving absolute density from inversion results and well data would significantly advance our understanding of an area and potentially drive up exploration activity. This progression would be the next phase in refining our workflow.

Acknowledgements

The authors would like to thank PGS for permission to publish this paper and for providing the datasets used in this study. We would also like thank the Oil and Gas Corporation of Newfoundland and Labrador (OilCo) for its support and fruitful discussions.

References

Chemingui, N., Yang, Y., Ramos-Martinez, J., Huang, G., Whitmore, D., Crawley, S., Klochikhina, E. and Arasanipalai, S. [2023]. Simultaneous Inversion of velocity and angle-dependent reflectivity. *Third International Meeting for Applied Geoscience & Energy, Expanded Abstracts.*

McCallum, D.S., Carter, J.E., Cameron, D.E. and Mitchell, V. [2017]. *A revised distribution of Mesozoic sediments and its implications on play type elements and interpreted leads within the Orphan basin, offshore Newfoundland and Labrador, Canada*. AAPG/SEG International Conference & Exhibition 2017.

Ramos-Martinez, J., Crawley S., Zou, Z., Valenciano, A.A., Qui, L. and Chemingui, N. [2016]. A Robust Gradient for Long Wavelength FWI Updates. *78th Conference and Exhibition, EAGE*, *Extended Abstracts,* SRS2.

Whitmore, N.D. and Crawley, S. [2012]. Applications of RTM inverse scattering imaging conditions. *SEG Technical Program, Expanded Abstracts*: 1-6.

Whitmore, N.D., Ramos-Martinez J., Yang, Y. and Valenciano A.A. [2021]. Full wavefield modeling with vector reflectivity. *83rd Annual International Conference and Exhibition*, *EAGE*, *Extended Abstracts*.

Yang, Y., Ramos-Martinez, J., Whitmore, N.D., Huang, G. and Chemingui, N. [2022]. Simultaneous inversion of velocity and reflectivity. *First International Meeting for Applied Geoscience & Energy*, *Expanded Abstracts.*